FULL PAPER

Dalton
www.rsc.org/dalton

Electrochemical and chemical oxidation of the antitumour agent $[Pt\{((p\text{-}HC_6F_4)NCH_2)_2\}(py)_2]$ – detection of platinum(III) intermediates

Dayna N. Mason,[a] Glen B. Deacon,[a] Lesley J. Yellowlees[b] and Alan M. Bond*[a]

[a] *School of Chemistry, P.O. Box 23 Monash University, Victoria, 3800, Australia. E-mail: Alan.Bond@sci.monash.edu.au*

[b] *School of Chemistry, The University of Edinburgh, West Mains Road, Edinburgh, UK EH9 3JJ*

Received 4th November 2002, Accepted 16th December 2002
First published as an Advance Article on the web 4th February 2003

The electrochemical (platinum and glassy carbon electrodes, cyclic and rotating disk electrode voltammetry, bulk electrolysis, voltammetric simulation) and chemical oxidation (NO^+) of the organoamidoplatinum(II) complex, $[Pt\{((p\text{-}HC_6F_4)NCH_2)_2\}(py)_2]$, has been studied in acetonitrile and acetone. The initial process is a complicated function of concentration, temperature, and method of oxidation. The products formed have been probed by *in situ* spectroelectrochemical techniques (UV/Visible and EPR spectroscopy), and *ex situ* by ^1H, ^{19}F and ^{195}Pt NMR spectroscopy and electrospray mass spectrometry. Under conditions of cyclic voltammetry, the initial oxidation process (at high concentration) is an overall irreversible one-electron process, complicated by crossover of current on the reverse scan. This and many (but not all) features are simulated by a sequence of electron transfer steps and coupled chemical reactions which requires the formation of two structurally different dinuclear intermediates. Regeneration of $[Pt\{((p\text{-}HC_6F_4)NCH_2)_2\}(py)_2]$ by reduction is possible under short timescale conditions, but not long timescale conditions, implying that the finally observed product from long timescale experiments may be oligomeric. The observation of moderately stable diamagnetic diplatinum(III) compounds is attributed to the formation of bridged complexes containing Pt–Pt bonds. Oxidation of all platinum(III) intermediates gives rise to the same or very closely related platinum(IV) complexes. Features of the organoamide ligand that enable the formation of moderately stable platinum(III) complexes are considered.

Introduction

N,N′-Bis(polyfluorophenyl)ethane-1,2-diaminato(2^-)dipyridineplatinum(II) complexes,[1,2] **1**, are a unique class of air stable organoamides (*cf.* exceptionally moisture-sensitive $Pt(NHCH_2)_2$, $Pt(NRCH_2)_2$bpy (bpy = 2,2′-bipyridyl)[3,4]), which have substantial antitumor activity.[5–9] In view of the increasing interest in platinum(IV) prodrugs, of which CHIP, **2**, and JM216, **3**, are typical representatives,[10,11] and the possibility that use of compounds in this oxidation state may represent a way of reducing side effects,[12] a systematic study of the synthesis and biological testing of platinum(IV) complexes has been initiated in these laboratories.[12,13] Initially, relatively inert organoplatinum(II) species were examined, where the oxidation functionalisation chemistry developed for JM216 and their analogues[14,15] may be readily adapted, giving *trans*-dihydroxo- and *trans*-dicarboxylato-platinum(IV) analogues. For the less robust and more biologically active complexes, such as $[Pt\{((p\text{-}HC_6F_4)NCH_2)_2\}(py)_2]$, a systematic study of the electrochemical oxidation seemed an invaluable precursor to attempted syntheses of the platinum(IV) analogues. These results are now presented and include the perhaps surprising detection of platinum(III) intermediates rather than the direct formation of the expected platinum(IV) moieties.

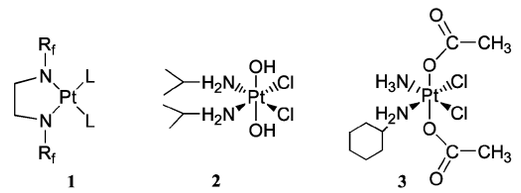

1

2

3

1: L = py, R_f = *p*-HC_6F_4, C_6F_5, *p*-BrC_6F_4, *p*-IC_6F_4, *p*-MeC_6F_4, *p*-$C_6F_5C_6F_4$, 2,3,5-$F_3C_6H_2$, *p*-$O(H)CC_6F_4$, *p*-$MeOC_6F_4$; L = tmpy, R_f = *p*-HC_6F_4. **2**: CHIP. **3**: JM-216.

Experimental

Chemicals and reagents

$[Pt\{((p\text{-}HC_6F_4)NCH_2)_2\}(py)_2]$ and $[Pt\{((p\text{-}HC_6F_4)NCH_2)_2\}(py)_2(OH)_2]$ were synthesised according to literature methods,[16,17] and were characterised by ^1H and ^{19}F NMR spectroscopy.

Electrolytes were prepared by literature methods[18] and the absence of electroactive impurities was confirmed by voltammetry.

Acetonitrile (Aldrich) was of HPLC grade, and used as received. Acetone (BDH) was refluxed over and distilled from potassium permanganate and stored under a nitrogen atmosphere over molecular sieves.

$NOPF_6$ and $NOBF_4$ were purchased from Aldrich and handled under an inert atmosphere.

Instrumentation

^1H and ^{19}F NMR spectra were obtained using a Bruker DPX300 spectrometer, whilst ^{195}Pt NMR spectra were obtained using a Bruker DRX500 instrument. Proton and fluorine chemical shifts are in ppm from internal $SiMe_4$ and $CFCl_3$ respectively. Phosphorus chemical shifts are in ppm from external H_3PO_4. Platinum chemical shifts were referenced to Na_2PtCl_6 by setting an external sample of K_2PtCl_4 in D_2O to −1620 ppm.

UV/Visible spectra were recorded using a Cary 5 spectrophotometer, running on Varian OS2 software. Molar (decadic) absorption coefficients are given in units mol^{-1} dm^3 cm^{-1}.

Electrospray mass spectra were obtained with a Micromass Platform benchtop QMS with an electrospray source and methanol spray solvent. Solutions of analyte in acetonitrile were introduced into the machine by an autosyringe.

EPR spectra were recorded on a Bruker [X-band] ER 200D instrument running at 9.49 GHz and fitted with a variable temperature unit.

DOI: 10.1039/b210815a

Electrochemical techniques

Voltammetric measurements were typically obtained with solutions of compound in acetone or acetonitrile with 0.1 M Bu_4NPF_6, Bu_4NBF_4 or Bu_4NClO_4 as the electrolyte using a MacLab(4e) computer controlled electrochemical system (AD Instruments Pty Ltd, Castle Hill, Australia). For conventional cyclic voltammetric experiments, the working electrode was either a glassy carbon (GC) disk (0.67 or 1.3 mm radius) or a platinum disk (0.49 mm radius), whilst rotating disk electrode (RDE) experiments were recorded using a Metrohm 628-10 RDE apparatus (Metrohm Ltd., Switzerland) with a GC working electrode (1.4 mm radius). The auxiliary electrode was either a platinum wire or a glassy carbon rod, and the reference electrode was a Ag/Ag^+ (0.1 M $AgNO_3$ in acetonitrile) separated from the test solution by a salt bridge. For bulk electrolysis experiments, a BAS 100A electrochemical analyzer (Bioanalytical Systems, West Lafayette, IN) was utilised, and both the working electrode and the auxiliary electrodes were platinum gauze, with the auxiliary electrode separated from the test solution by a glass frit. The reference electrode was Ag/Ag^+ as above. The reversible voltammetry for oxidation of an approximately 5 mM ferrocene (Fc) solution in the same solvent was used as a reference redox couple, and all potentials are quoted relative to the Fc/Fc^+ potential scale. Solutions were purged with solvent-saturated nitrogen prior to undertaking voltammetric measurements and then maintained under an atmosphere of nitrogen for the duration of the experiments. *In situ* UV/Visible experiments were performed in a 1 mm thick optically transparent thin-layer cell, with a platinum gauze working electrode, a platinum wire auxiliary electrode (separated from the test solution by a glass frit), and the Ag/Ag^+ reference electrode as above. *In situ* EPR experiments were performed in a standard quartz EPR flat cell with a platinum gauze working electrode in the flat section. The auxiliary electrode was a platinum wire, and the reference electrode was Ag/AgCl.

Software packages

EPR spectra were simulated using WINEPR SimFonia software.[19] Frozen glass spectra were simulated by the EPSRC multicentre EPR service in Manchester. Voltammetric simulations were carried out using DigiSim software.[20]

Results and discussion

The electrochemistry of $[Pt\{((p\text{-}HC_6F_4)NCH_2)_2\}(py)_2]$ is a complicated function of concentration, electrolyte, temperature and technique. In order to immediately convey the major features, an initial overview is presented using conditions where only three primary processes are detected at a GC electrode, under both transient (cyclic voltammetry at a stationary electrode) and near steady-state (rotated disk electrode) voltammetric conditions. Fig. 1a shows a transient cyclic voltammogram of a 10 mM $[Pt\{((p\text{-}HC_6F_4)NCH_2)_2\}(py)_2]$ solution in acetonitrile in the positive and negative potential range *vs*. Fc/Fc^+, using a scan rate of 1000 mV s^{-1} and a GC macrodisk electrode. A near steady-state experiment at a rotating disk electrode is shown in Fig. 1b. Clearly, under conditions relevant to Fig. 1 there are two well-resolved oxidation processes and a reduction process – referred to as primary Processes 1, 2 and 3 respectively. Less well defined reductive processes are also detected at very negative potentials (not described). The rotating disk electrode experiment implies that all three major processes have the same number of electrons in the overall charge transfer process since all responses have similar mass transport controlled limiting currents.

Under conditions of cyclic voltammetry and at all scan rates examined (100–5000 mV s^{-1}), all three processes depicted in Fig. 1 are chemically irreversible at room temperature for all analyte concentrations examined (0.5–10 mM), in both

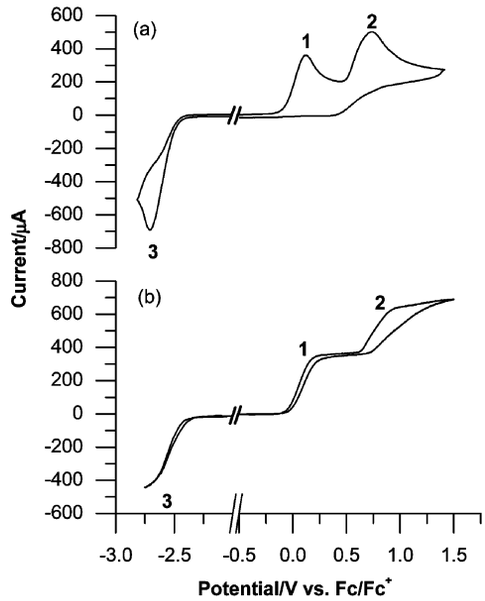

Fig. 1 Voltammetry of 10 mM $[Pt\{((p\text{-}HC_6F_4)NCH_2)_2\}(py)_2]$ in acetonitrile (0.1 M Bu_4NBF_4) at 20 °C at a GC electrode (1.3 mm radius). (a) Cyclic voltammetry using a scan rate of 1000 mV s^{-1}. (b) RDE voltammetry using a scan rate of 10 mV s^{-1} and an electrode rotation rate of 500 rpm.

acetonitrile and acetone, and with all electrolytes (0.1 M Bu_4NBF_4, Bu_4NPF_6, Bu_4NClO_4). However, at −78 °C in acetone, under conditions of cyclic voltammetry the reduction process shows a small amount of chemical reversibility at scan rates greater than 1000 mV s^{-1}. Only the two chemically irreversible oxidations could be observed at platinum electrodes under the experimental conditions of Fig. 1. Since only the oxidation of the platinum(II) compound is of interest in future synthetic investigations of antitumor platinum(IV) complexes, the presumed platinum(II) to platinum(I) reduction process will not be considered further.

Voltammetry

The simplest voltammetric behaviour is observed at $[Pt\{((p\text{-}HC_6F_4)NCH_2)_2\}(py)_2]$ concentrations in the mM range, with 0.1M supporting electrolyte, and when GC electrodes are used. Thus, in order to define and summarise key mechanistic details of the two major oxidation processes, initial discussions will focus on experiments undertaken under these conditions.

(a) Rotating disk electrode experiments. At a rotated GC electrode with a scan rate of 10 mV s^{-1} and with rotation rates in the range 500 to 3000 rpm, almost complete overlap of voltammetric responses for Process 1 is detected in both positive and negative scan directions (Fig. 2a). This occurs irrespective of the initial scan direction, provided the potential is switched (or commenced) prior to the onset of Process 2. This implies that no significant surface interactions occur under these conditions. Unlike Process 1 in Fig. 2a, the forward and reverse scans of Process 2 do not overlap (Fig. 1b), suggesting significant surface interaction takes place at more positive potentials. It is this surface interaction which causes lack of overlap for Process 1 in Fig. 1b. However, the equivalent magnitude of the limiting current, I_L, implies Process 2 involves the same overall number of electrons in the charge transfer process as Process 1.

In order to determine the number of electrons responsible for Processes 1 and 2, the RDE voltammetry of the platinum(IV) dihydroxide complex, $[Pt\{(p\text{-}HC_6F_4)NCH_2)_2\}(py)_2(OH)_2]$, was examined. Dihydroxoplatinum(IV) organometallic complexes and platinum(IV) porphyrins commonly undergo irreversible two-electron reduction.[12,21] Coulometric studies of the

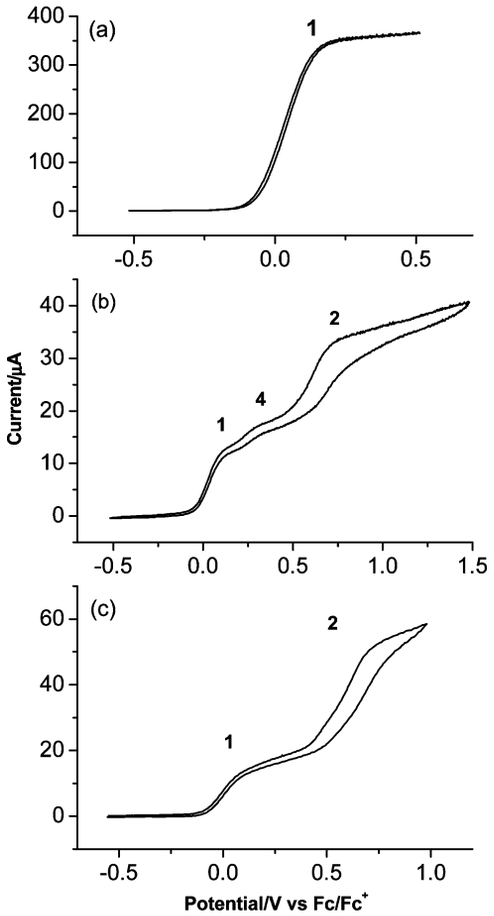

Fig. 2 RDE voltammetry of [Pt{((*p*-HC_6F_4)NCH_2)$_2$}$(py)_2$] at 20 °C at a GC electrode (1.3 mm radius) using a scan rate of 10 mV s^{-1} and an electrode rotation rate of 500 rpm. (a) 10 mM solution in acetone (0.1 M Bu_4NPF_6). (b) 0.5 mM solution in acetonitrile (0.1 M Bu_4NClO_4). (c) 0.5 mM solution in acetonitrile (0.1 M Bu_4NBF_4).

reduction of [Pt{(*p*-HC_6F_4)NCH_2)$_2$}$(py)_2(OH)_2$] is consistent with the reaction in eqn. (1).

$$[Pt^{IV}\{((p\text{-}HC_6F_4)NCH_2)_2\}(py)_2(OH)_2] + 2e^- \rightarrow \text{products} \quad (1)$$

The molecular weights of both platinum complexes are similar (707 g mol^{-1} and 714 g mol^{-1} for the platinum-(II) and -(IV) analogues respectively), so it is reasonable to assume the diffusion coefficients would also be similar. At 5 mM in acetonitrile (0.1 M Bu_4NBF_4) at a scan rate of 10 mV s^{-1} and a rotation rate of 1000 rpm, I_L of the reduction of [Pt{(*p*-HC_6F_4)NCH_2)$_2$}-$(py)_2(OH)_2$] is 500 μA, whereas under these conditions, Process 1 has I_L of 245 μA. This indicates that Processes 1, and hence 2 and 3 are overall one-electron processes. Further evidence of this was obtained from bulk electrolysis (BE) experiments (see later).

At concentrations greater than approximately 2.5 mM, I_L is linearly dependent on the square root of the rotation rate (500 to 3000rpm) and concentration, and obeys the Levich Equation (eqn. (2)

$$I_L = 0.620nFAD_0^{2/3}\omega^{1/2}\nu^{-1/6}c_0^* \quad (2)$$

where I_L = limiting current (A), n = number of electrons, F = Faraday's constant (96,485 C mol^{-1}), A = electrode area (cm^2), D_0 = diffusion coefficient (cm^2 s^{-1}), ω = angular frequency of rotation (s^{-1}), ν = kinematic viscosity (cm^2 s^{-1}), and c_0^* = concentration (mol cm^{-3})). At lower concentrations, a distinctly different dependence on these variables is observed. The diffusion coefficient of [Pt{((*p*-HC_6F_4)NCH_2)$_2$}$(py)_2$] was calculated to be $1\pm0.1 \times 10^{-5}$ cm^2 s^{-1} using the Levich Equation and concentrations ≥ 2.5 mM, assuming a one-electron oxidation process.

Table 1 GC rotating disk voltammetric data associated with Process 1 for solutions of [Pt{((*p*-HC_6F_4)NCH_2)$_2$}$(py)_2$] in acetone (0.1 M Bu_4NPF_6)

Rotation rate	Conc./mM	$E_{½}$/mV	$E_{3/4} - E_{1/4}$/mV	I_L/μA
500 rpm	0.5	48	59	11.7[a]
	1.0	35	80	39
	5.0	35	88	171
	10.0	81	115	350
2500 rpm	0.5	70	62	22.9[a]
	1.0	58	80	87.6
	5.0	81	112	379
	10.0	98	175	770

[a] Minor process appears between Processes 1 and 2.

The halfwave potential ($E_{½}$) of Process 1 at a RDE is dependent on rotation rate, concentration and electrolyte. At low [Pt{((*p*-HC_6F_4)NCH_2)$_2$}$(py)_2$] concentrations, the electrolyte dependence is most obvious. The use of Bu_4NPF_6 or Bu_4NClO_4 reveals an extra process (Process 4) between Processes 1 and 2, whilst the use of Bu_4NBF_4 introduces additional complexity into Process 2. Fig. 2b and c show representative voltammograms. Where Process 4 is detected, I_L data suggest that oxidation Processes 1 and 2 now involve an overall less than one electron transfer process, but that the sum of Processes 1 and 4 corresponds to an overall one-electron step. Table 1 gives data obtained with the RDE technique in acetone (0.1 M Bu_4NPF_6) with rotation rates of 500 and 2500 rpm. Clearly, there are at least two competing mechanisms associated with Process 1, one (n < 1) favoured at low concentrations and long time domains, and the other (n = 1) at high concentrations and short time domains.

(b) Cyclic voltammetry. At high concentrations of [Pt{((*p*-HC_6F_4)NCH_2)$_2$}$(py)_2$] and when using cyclic voltammetry, switching the potential immediately after the first oxidation process leads to the detection of a crossover region at the foot of Process 1 and a chemically reversible couple at about −800 mV (Process 5) on the reverse scan and in subsequent cycles of the potential (Fig. 3a). When scanning to very negative potentials, an irreversible reduction process (Process 6) is observed, as shown in Fig. 3b, whose peak potential on the first cycle is very different to that of following cycles. Table 2 gives peak potentials (E_p) of Processes 1, 2 and 5 in acetonitrile (0.1 M Bu_4NBF_4). The use of 0.1 M Bu_4NPF_6 or Bu_4NClO_4 as an electrolyte gives similar data. Cyclic voltammetric data in acetone are also similar to those obtained in acetonitrile.

When the potential is switched between Processes 1 and 2, repetitive cycling causes Process 1 to diminish in height. However, scanning through Process 6 makes Process 1 essentially independent of cycling. At all scan rates and conditions examined for the 10 mM solution, Process 5 is well defined, provided the potential is switched prior to the onset of Process 2. Data obtained for Processes 1 and 5 measured with a GC electrode in acetonitrile as a function of electrolyte are summarised in Table 3. The chemically reversible Process 5 is very insensitive to the experimental conditions summarised in Table 3, whereas Process 1 is slightly dependent and the biggest variation occurs with Process 6.

The $\Delta E_p(5)$ value for Process 5 is close to that found for the known reversible one-electron oxidation of ferrocene under the same set of conditions, which implies this is a chemically and electrochemically reversible one-electron process. The fact that $\Delta E_p(5)$ values are ≥ 60 mV and increase with scan rate and concentration implies that a small amount of uncompensated resistance is present. As the concentration of [Pt{((*p*-HC_6F_4)-NCH_2)$_2$}$(py)_2$] is decreased, the extent of chemical reversibility

Table 2 Selected cyclic voltammetric data for solutions of [Pt{((*p*-HC_6F_4)NCH_2)$_2$}(py)$_2$] in acetonitrile (0.1 M Bu_4NBF_4)

Electrode, Conc./mM	Scan rate/ mV s^{-1}	$E_p(1)$/ mV	$I_p(1)$/μA	$E_p(2)$/mV	$I_p(2)$/μA	$E_p^{ox}(5)$[a]/mV	$I_p^{ox}(5)$[a]/μA	$E_p^{red}(5)$[a]/mV	$I_p^{red}(5)$[a]/μA	$\Delta E_p(5)$[a,b]/ mV
GC[c], 1.0	100	23	12.7	553	19.1	NO[d]	NO	NO	NO	NO
	500	33	26.6	573	44.1	NR[e]	NR	−832	3.50	NR
	1000	38	37.2	573	50.3	−767	1.59	−822	3.24	55
GC[c], 5.0	100	−31	84.2	498	132	NR	NR	−818	0.6	NR
	500	11	189	570	270	−763	2.34	−853	3.0	90
	1000	67	251	722	376	−784	4.30	−895	6.0	111
GC[c], 10.0	100	3	138	543	140	NR	NR	−822	6.43	NR
	500	50	262	580	213	−775	5.5	−835	27.5	60
	1000	83	346	633	311	−737	20.3	−852	53.6	115
Pt, 1.0	100	68	1.80	558	2.13	NO	NO	NO	NO	NO
	500	83	3.40	673	5.49	NR	NR	−817	0.40	NR
	1000	88	4.96	648	8.33	NR	NR	−837	0.34	NR
Pt, 5.0	100	20	8.60	570	7.32	NR	NR	−805	0.56	NR
	500	70	17.1	705	14.2	−745	0.84	−810	2.03	65
	1000	95	20.0	695	23.3	−730	2.83	−840	3.59	110
Pt, 10.0	100	7	19.3	558	16.8	NR	NR	−822	0.50	NR
	500	48	29.0	613	28.9	−777	2.56	−832	2.66	55
	1000	68	40.7	643	42.2	−747	2.68	−847	4.60	100

[a] Data obtained when potential is switched between Processes 1 and 2. [b] $\Delta E_p(5) = E_p^{ox}(5) - E_p^{red}(5)$. [c] r = 1.3 mm. [d] NO = Not observed. [e] NR = Not reversible.

Table 3 Cyclic voltammetric data at a scan rate of 500 mV s^{-1} for 5 mM solutions of [Pt{((*p*-HC_6F_4)NCH_2)$_2$}(py)$_2$] with various electrolytes at a GC electrode[a]

Electrolyte	$E_p(1)$/mV	$E_p^{ox}(5)$/mV	$E_p^{red}(5)$/mV	$E_p(6)$[b]/mV	$E_p(6)$[c]/mV
Bu_4NPF_6	16	−786	−870	−2195	NA[d]
Bu_4NBF_4	50	−763	−853	−2377	−2383
Bu_4NClO_4	48	−772	−862	−1992	−1767

[a] The potential is switched prior to the onset of Process 2. [b] First scan. [c] Third scan. [d] Not acquired.

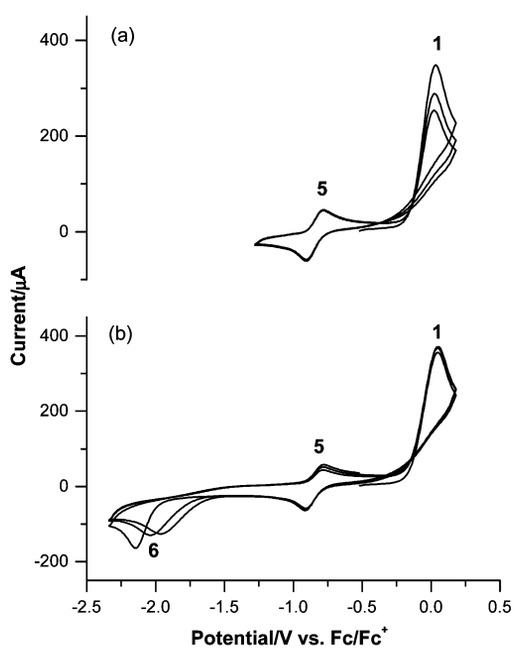

Fig. 3 Cyclic voltammetry (3 cycles of potential) at a GC electrode (1.3 mm radius) of 10 mM [Pt{((*p*-HC_6F_4)NCH_2)$_2$}(py)$_2$] in acetonitrile (0.1M Bu_4NBF_4) at 20 °C. Using an initial potential of −500 mV *vs.* Fc/Fc^+ and a scan rate of 1000 mV s^{-1}. (a) Switching potential at −1280 mV. (b) Switching potential at −2340 mV.

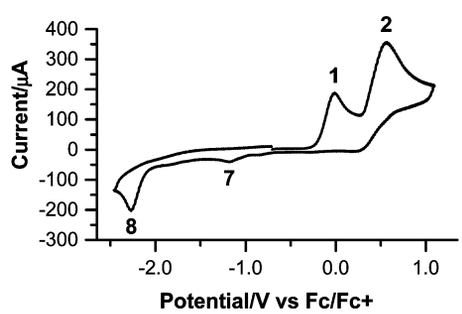

Fig. 4 Cyclic voltammetry encompassing both Processes 1 and 2 of 5 mM [Pt{((*p*-HC_6F_4)NCH_2)$_2$}(py)$_2$] in acetonitrile (0.1 M Bu_4NBF_4) at 20 °C at a GC electrode (r = 1.4 mm) using a scan rate of 1000 mV s^{-1}.

of Process 5 also decreases. At 0.5 mM, Process 5 is undetectable, even with a scan rate of 5000 mV s^{-1}.

Scanning to potentials more positive than Process 2 essentially removes any evidence of Processes 5 and 6 on the reverse scan. Additionally, as Fig. 4 illustrates, we see a small process at about −1200 mV (Process 7), and a more well-defined process at about −2300 mV (Process 8). The exact details of Processes 7 and 8 are also highly dependent on experimental conditions (scan rate, concentration, electrolyte).

Cyclic voltammetry of [Pt{((*p*-HC_6F_4)NCH_2)$_2$}(py)$_2$] at low concentration reveals Process 4. Examination of the cyclic voltammogram in acetone at low temperatures (−78 °C) reveals some additional responses relative to those seen at 20 °C, discussed above. Process 1 remains very clean, while a shoulder appears just prior to Process 2 (at 458 mV), which is then replaced by two small responses in the same potential region upon repetitive cycling. When the potential is reversed immediately following Process 1, there is now relatively little formation of the Process 5 reduction peak, and the appearance of a chemically reversible process at $E_{½}$ −1490 mV suggests different intermediates are detected relative to those at room temperature. These intermediates will not be considered further.

Bulk electrolysis

Bulk electrolysis (BE) was undertaken at a range of [Pt{((*p*-HC_6F_4)NCH_2)$_2$}(py)$_2$] concentrations, supporting electrolytes and in both acetone and acetonitrile. Cyclic and RDE

voltammograms were taken before and after the experiment. When the potential is held between Processes 1 and 2, Process 1 always disappears completely (voltammetric detection) after exhaustive electrolysis and at all concentrations a well defined oxidation process (Process 9) appears in a similar position to Process 2 (see Fig. 5). At a concentration of 5 mM, new reduction processes appear at −1100 mV and −2350 mV on the reverse scan of the cyclic voltammograms (Processes 10 and 11 respectively), which are at similar positions to Processes 7 and 8 (see Fig. 4). Under no conditions is Process 5 observed after BE. However, following electrolysis of 1 mM solutions, a well defined reduction process can be observed at −1000 mV under RDE conditions (Process 12, see Fig. 6). This process leads to the regeneration of $[Pt\{((p\text{-}HC_6F_4)NCH_2)_2\}(py)_2]$ under CV condtions. The position and shape of reduction responses from bulk material varies significantly with time and concentration, especially in the negative potential region. With a 5 mM solution, coulometric determination of BE experiments indicates Process 1 is always slightly less than a one-electron transfer process (*i.e.* $n = 0.90 \pm 0.07$).

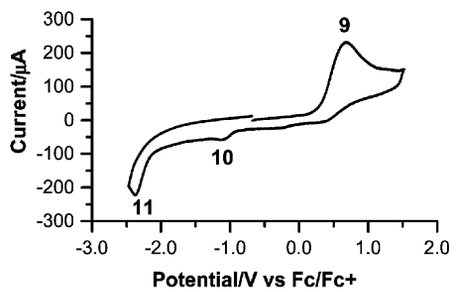

Fig. 5 Cyclic voltammogram following the controlled potential electrolysis of a 5 mM solution of $[Pt\{((p\text{-}HC_6F_4)NCH_2)_2\}(py)_2]$ in acetonitrile (0.1 M Bu_4NBF_4) at 20 °C at a GC electrode (r = 1.4 mm) using a scan rate of 1000 V s^{-1}.

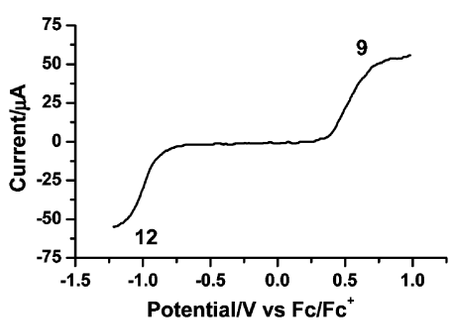

Fig. 6 RDE voltammogram following the controlled potential electrolysis of a 1 mM solution of $[Pt\{((p\text{-}HC_6F_4)NCH_2)_2\}(py)_2]$ in acetonitrile (0.1 M Bu_4NPF_6) at 27 °C at a GC electrode (r = 1.4 mm) using a rotation rate of 500 rpm and a scan rate of 10 mV s^{-1}.

If the 1 mM solution of $[Pt\{((p\text{-}HC_6F_4)NCH_2)_2\}(py)_2]$ is allowed to age in air, the number of coulombs consumed in a BE experiment for the first process decreases. Furthermore, with voltammetric monitoring, it is noted that the second wave (Process 2/9) grows at the expense of the first. Over a period of two days, $\frac{2}{3}$ of the starting material was lost, highlighting the importance of both studying only fresh solutions, and also that reaction with molecular oxygen and/or moisture appears to parallel that of BE.

If a BE experiment is undertaken at a more positive potential than Process 2, both Processes 1 and 2/9 disappear, so no voltammetrically active species can be detected in the potential range −2500 to 800 mV. Coulometric determinations for this BE experiment at very positive potentials were very much a function of concentration, but always gave $n \geq 2$.

Optically transparent thin layer electrochemistry (OTTLE)

Examination of a 1 mM solution of $[Pt\{((p\text{-}HC_6F_4)NCH_2)_2\}(py)_2]$ in acetonitrile by UV/Visible spectroscopy reveals three major bands – a charge transfer band at 230 nm (ε = 22800), a pyridine-to-platinum charge transfer band at 299 nm (ε = 15700) and a complicated ligand-to-ligand charge transfer band at 365 nm (ε = 13000).[22] In this spectroelectrochemical experiment, when the potential is held between the Processes 1 and 2 and the electronic spectra is measured as a function of time, the charge transfer band at 230 nm disappears, and the other bands reduce in size (295 nm [ε = 10900], 365 nm [ε = 300]) (see Fig. 7a). During the first three minutes, the appearance of an isosbestic point at about 225 nm suggests a clean electrochemical reaction, with only two species present in the solution,[23] although caution is advised in reaching this conclusion.[24] The loss of the isosbestic point suggests that a further chemical reaction takes place on longer timescales. The finally formed oxidised species is moderately stable in solution (10 minutes timescale). Recovery of 90–95% of the original $[Pt\{((p\text{-}HC_6F_4)NCH_2)_2\}(py)_2]$ is achievable by immediate reduction at a potential of −1200 mV (provided the electrolyte used is not a perchlorate, when recovery is only 50–60%). Recovery of all spectral features associated with the starting material occurs, as seen in Fig. 7b, and when Bu_4NPF_6 is used as the electrolyte, an isosbestic point is evident at 225 nm. Similar results are obtained when the temperature is held at 0 °C.

These recovery results suggest little decomposition involving complete loss of ligands is associated with the one-electron oxidation when the supporting electrolyte is Bu_4NBF_4 or

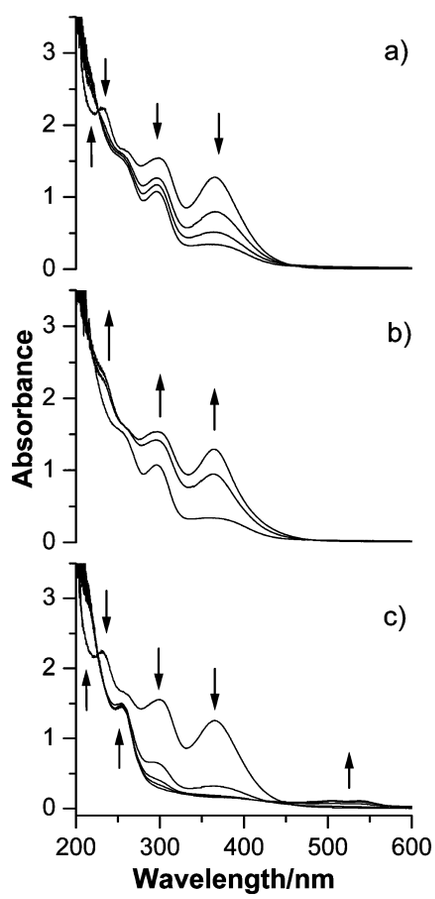

Fig. 7 Changes of the UV/Visible spectrum of a 1 mM solution of $[Pt\{((p\text{-}HC_6F_4)NCH_2)_2\}(py)_2]$ in acetonitrile (0.1 M Bu_4NBF_4) in an OTTLE cell at 20 °C. (a) Potential held between the first and second oxidation responses. (b) Reduction of oxidised solution to recover original platinum species. (c) Oxidation of fresh solution when the potential is held more positive than Process 2.

Bu_4NPF_6. If, for example, the organoamide ligand or the pyridine irreversibly dissociated from the platinum metal centre during oxidation (with protonation of the former), then recovery of the initial spectrum would not be probable.

If the potential is held at a value more positive than Process 2, the disappearance of the characteristic [Pt{((*p*-HC_6F_4)-$NCH_2)_2$}$(py)_2$] bands is much faster, leaving only one major spectral feature at 255 nm (ε = 15100) and a broad low intensity band at 450 to 570 nm (see Fig. 7c). This time, reduction of the solution at −1200 mV fails to regenerate the initial spectrum. Similar results (for wavelengths ≥ 300 nm) are obtained when acetone is used as a solvent

In situ EPR spectroelectrochemistry

By performing partial electrolysis on a high concentration (50 mM) solution of [Pt{((*p*-HC_6F_4)$NCH_2)_2$}$(py)_2$] in acetonitrile (0.1 M Bu_4NBF_4) in the cavity of an EPR spectrometer, at potentials between Processes 1 and 2, a moderately stable paramagnetic species of significant concentration was detected. Fig. 8a shows a comparison of experimental and simulated results with a *g* value of 2.004, which is close to the value of a free electron (2.0023). The coupling of the signal indicates the electron occupies an orbital based on two nitrogen atoms and the platinum metal centre. EHMO (Extended Hückel Molecular Orbital) calculations suggest that the nitrogens belong to the organoamide ligand, as the HOMO of the molecule is primarily located on the platinum and the two organoamide nitrogen donor atoms (the rest is found on the fluorophenyl rings).[22] Detection of the EPR active species at room temperature requires high concentrations of [Pt{((*p*-HC_6F_4)$NCH_2)_2$}$(py)_2$] and carefully selected electrolysis conditions (potential and time). After generation of this species, the solution was frozen to give the glass EPR spectrum, shown in Fig. 8b. These results establish that the mono-oxidised species is anisotropic, and only platinum hyperfine coupling is observed. The glass *g* values of $g1$ = 2.046, $g2$ = 2.000, and $g3$ = 1.958 average well to the isotropic *g* value as do the Pt hyperfine coupling constants A_1 = 72.5 G, A_2 = 100 G and A_3 = 25 G to A_{iso}. In addition to these values the simulation in Fig. 8b used line widths of w_1 = 20 G, w_2 = 15 G and w_3 = 40 G. The EPR result indicates that the site of oxidation is associated with an orbital that has between 10 and 20% platinum character.

Chemical oxidation

The known one electron oxidant, NO^+ as nitrosonium hexafluorophosphate ($NOPF_6$) or nitrosonium tetrafluoroborate ($NOBF_4$), was reacted with [Pt{((*p*-HC_6F_4)$NCH_2)_2$}$(py)_2$]. The advantage of chemical oxidation is that the electrolyte will be absent, which simplifies the use of NMR spectroscopic and ESMS techniques for product characterisation. Addition of one equivalent of $NOPF_6$ or $NOBF_4$ to a 10 mM solution of the analyte in acetonitrile or acetone caused the bright yellow solution to immediately change colour to light yellow. Over a period of 2 hours, the solution progressively changed colour to orange, and decomposition of the complex was detected by ^{19}F NMR spectroscopy (evidence of protonated non-coordinated organomide ligand). As a result, all NMR spectra were collected within the hour following chemical oxidation.

Oxidation by one mole equivalent of $NOPF_6$ (one electron) in acetonitrile yielded a similar UV/Visible spectrum to that obtained when the potential is held between Processes 1 and 2 (359 nm [ε = 700]). When $NOPF_6$ is added in half equivalent lots to a 10 mM solution of [Pt{((*p*-HC_6F_4)$NCH_2)_2$}$(py)_2$], and the reaction is monitored voltammetrically as soon as practical (minutes timescale), Process 1 disappears at the 1 : 1 ratio in a similar manner to that observed during bulk electrolysis at a potential between Processes 1 and 2 (see Fig. 9). Additionally, a major oxidation process is still detected at a higher potential (Process 2/9), and a well-defined reduction wave at −1100 mV

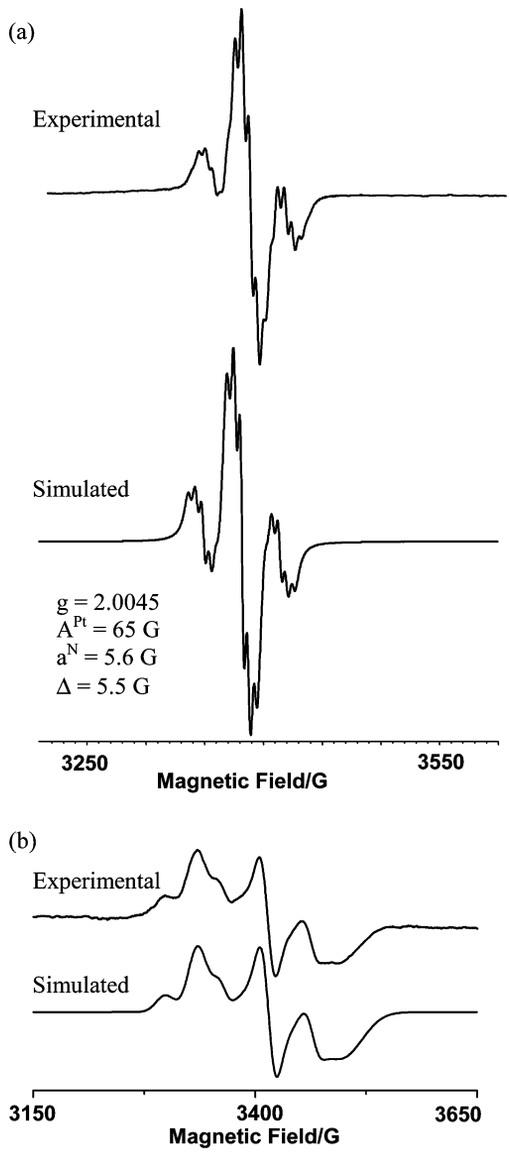

Fig. 8 *In situ* EPR spectrum of [Pt{((*p*-HC_6F_4)$NCH_2)_2$}$(py)_2$], recorded during oxidation in acetonitrile (0.1 M Bu_4NBF_4). (a) 273 K. (b) 77 K.

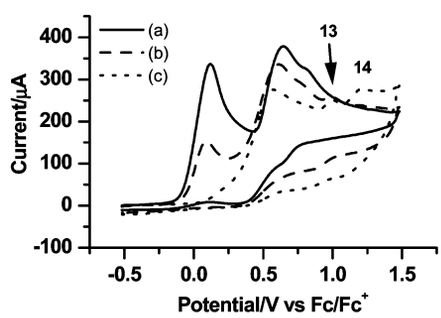

Fig. 9 (a) Cyclic voltammogram of a 10 mM solution of [Pt{((*p*-HC_6F_4)$NCH_2)_2$}$(py)_2$] in acetone (0.1 M Bu_4NPF_6) at a GC electrode (r = 1.4mm) with a scan rate of 500 mV s^{-1}. (b) Response following addition of half an equivalent of $NOPF_6$. (c) Following subsequent addition of half an equivalent of $NOPF_6$ (one equivalent total).

(Process 12) can be observed. Cyclic voltammograms that encompassed the potential region of reduction Process 12 led to regeneration of Process 1. The appearance of two new oxidation processes at a higher potential than Process 2/9 (Processes 13 and 14) can be attributed to the formation of non-coordinated protonated organoamide ligand (see also NMR Spectro-

scopy below). Interestingly, Processes 13 and 14 are not observed when one equivalent of the oxidant is added at once, emphasising the complexity of the oxidation.

Oxidation with two mole equivalents of the NO^+ eliminates Process 2/9, leaving no electrochemically detectable oxidation processes. However, stepwise addition of NO^+ in a series of 0.5 equivalents requires up to 4 equivalents to remove Process 2/9.

(a) NMR Spectroscopy. Oxidations of 10 mM solutions of $[Pt\{((p\text{-}HC_6F_4)NCH_2)_2\}(py)_2]$ in deuterated acetone by $NOPF_6$ and $NOBF_4$ have also been examined by ^1H, ^{19}F and ^{195}Pt NMR spectroscopy. The initial ^1H spectrum for $[Pt\{((p\text{-}HC_6F_4)NCH_2)_2\}(py)_2]$ has 5 distinct resonances.[2] The combination of the appearance of the (p-HC_6F_4) proton at 6.23 ppm (*cf*. the free protonated ligand value of 6.65 ppm[26]), the platinum satellites on the methylene resonance ($^3J_{Pt,H(CH2)}$ 29 Hz) and the lack of a NH peak (5.40 ppm for the free protonated ligand[26]) confirms the attachment of the organoamide ligand to the platinum. Three pyridine peaks appear in the range 7.2–8.7 ppm, with the H2,6(py) also showing platinum satellites ($^3J_{Pt,H(py)}$ 34 Hz). ^{19}F NMR spectroscopy reveals multiplets at −144.7 and −150.7 ppm due to the fluorocarbons on the organoamide ligand,[2] and ^{195}Pt NMR spectroscopy gives one broad signal at −2385 ppm (width at half height 1140 Hz).

Examination of the NMR spectra as soon as possible following oxidation by one equivalent of $NOPF_6$ or $NOBF_4$ indicates formation of similar products for both anions. The ^{195}Pt response was shifted to −2585 ppm (width at half height 1430 Hz), indicating the initial platinum species, $[Pt\{((p\text{-}HC_6F_4)NCH_2)_2\}(py)_2]$, was consumed and that a new platinum environment had been created. As there is only one response, this suggests the complex is symmetrical, with only one platinum environment.[27] It is difficult to predict the oxidation state of the platinum by its chemical shift, as this varies greatly with variance of ligands, solvent and temperature.[28–30] Generally, platinum(II) occurs at a lower frequency than the corresponding platinum(IV) analogue,[30–33] and available data do not provide a definitive region for the occurrence of platinum(III).

The ^{19}F responses have shifted to slightly higher frequency (−140 and −148 ppm) while retaining their one-to-one integration, which suggests both fluorocarbons are in the same environment and remain attached to the platinum (peak positions for the free protonated ligand are −142.2 and −160.4 ppm[26]). The peak-to-peak separation has increased compared with the platinum(II) starting material, which is unusual as oxidation to platinum(IV) generally causes a decrease in this peak-to-peak separation (see Table 4). These peaks are in similar positions to those recorded in non-deuterated solvent following oxidation by bulk electrolysis. Resonances attributable to the anion of the oxidant can be found as a singlet at −150.4 ppm for BF_4^- and a doublet at −71.6 ppm for PF_6^-. In the PF_6^- case, the hydrolysed anion, $PO_2F_2^-$, is also present, as a doublet at −80.1 in the ^{19}F NMR spectrum and a triplet at −13.5 ppm in the ^{31}P NMR spectrum with $^3J_{P,F}$ coupling of 950 Hz, which agrees with literature values.[34]

Table 4 Summary of the ^{19}F NMR chemical shifts of the organoamidoplatinum(II) complex and its oxidation products. Values are referenced to $CFCl_3$

Complex	F3,5/ppm	F2,6/ppm
$[Pt\{((p\text{-}HC_6F_4)NCH_2)_2\}(py)_2]$[a]	−144.7	−150.7
+ 1 equiv. $NOPF_6$	−140.3	−147.4
+ 1 equiv. $NOBF_4$	−140.1	−147.6
+ 2 equiv. $NOPF_6$	−139.5	−146.3
+ 2 equiv. $NOBF_4$	−138.0	−145.5(br)[b]
$[Pt\{((p\text{-}HC_6F_4)NCH_2)_2\}(py)_2(OH)_2]$[c]	−143.3	−143.5
$[Pt\{((p\text{-}HC_6F_4)NCH_2)_2\}(py)_2Cl_2]$[d]	−141.1	−142.8

[a] From ref. 2. [b] Broad signal. [c] From ref. 17. [d] From ref. 25.

Examination of the ^1H NMR spectrum confirms both ligands are present and in the expected ratio. A shift to higher frequency of all peaks is observed (see Table 5), which is indicative of the oxidation of the platinum organoamide complex, as illustrated by the dihydroxo- and dichloro-platinum(IV) analogues, where the (p-HC_6F_4) values for $[Pt\{((p\text{-}HC_6F_4)NCH_2)_2\}(py)_2(OH)_2]$ and $[Pt\{((p\text{-}HC_6F_4)NCH_2)_2\}(py)_2Cl_2]$ shift by 0.60 and 0.84 ppm respectively. However, the $^3J_{Pt,H}$ coupling constants for the chemically oxidised products are between those found for the platinum(II) and platinum(IV) analogues (Table 5), consistent with the formation of diplatinum(III) species.

Combination of this information indicates that chemical oxidation of high concentrations of $[Pt\{((p\text{-}HC_6F_4)NCH_2)_2\}(py)_2]$ is a clean one-electron reaction, producing one new diamagnetic (probably Pt^{II}) species. This species slowly decomposes to give the free protonated organoamide ligand and undetermined platinum species.

The ^{19}F NMR spectrum after oxidation by two equivalents of NO^+ is complicated, with three peaks observed, in a ratio of 1 : 3 : 2.6. The third peak is quite broad, which complicates the interpretation. This pattern suggests multiple products and/or non-symmetrical configuration of the resulting complex. The ^1H NMR spectrum reveals that the organoamide ligand and the pyridines are still attached to the platinum in the expected ratio.

(b) Electrospray mass spectrometry. Positive ion electrospray mass spectrometry (ESMS) of the solution following oxidation by one mole equivalent of $NOBF_4$ clearly reveals the formation of multinuclear platinum species, with peaks with correct isotope pattern at m/z 1502 attributed to the formation of a Pt(II)–Pt(III) ion, $[2M + BF_4 + H]^+$, where M is the complex $[Pt\{((p\text{-}HC_6F_4)NCH_2)_2\}(py)_2]$. The parent ion $[2M]^{2+}$ is not detectable and the major peak is at m/z 708, which corresponds to $[M + H]^+$. Likewise, the major peak for the oxidation by one mole equivalent of $NOPF_6$ is the $[M + H]^+$ peak at m/z 708. However, there is evidence of fragments with high molecular weights consistent with the formation of unassigned dinuclear platinum species, complicated by the hydrolysis of PF_6^-. When ESMS is performed on $[Pt\{((p\text{-}HC_6F_4)NCH_2)_2\}(py)_2]$, the major peak is also at m/z 708, but unlike the oxidized product, no signals at higher m/z values can be detected.

Table 5 Summary of the ^1H NMR chemical shifts of the organoamidoplatinum(II) complex and its oxidation products. Values are referenced to $SiMe_4$

	CH_2/ppm	p-H(C_6F_4)/ppm	H3,5(py)/ppm	H4(py)/ppm	H2,6(py)/ppm ($^3J_{Pt,H}$/Hz)
$[Pt\{((p\text{-}HC_6F_4)NCH_2)_2\}(py)_2]$[a]	3.17	6.24	7.25	7.84	8.61 (34)
+ 1 equiv. $NOPF_6$	3.49	7.00	7.47	7.94	8.89 (32)
+ 1 equiv. $NOBF_4$	3.50	7.01	7.44	7.90	8.86 (29)
+ 2 equiv. $NOPF_6$	4.12	7.35	7.52	8.00	9.00 (32)
+ 2 equiv. $NOBF_4$	3.90	7.40	7.57	8.03	8.98 (32)
$[Pt\{((p\text{-}HC_6F_4)NCH_2)_2\}(py)_2(OH)_2]$[b]	2.91	6.84	7.40	7.91	9.07 (21)
$[Pt\{((p\text{-}HC_6F_4)NCH_2)_2\}(py)_2Cl_2]$[c]	2.95	7.08	7.45	8.02	8.81 (16)

[a] From ref. 2. [b] From ref. 17. [c] From ref. 25.

Simulation of cyclic voltammetry

Simulations of voltammograms were undertaken, in order to assist in the elucidation of the mechanism of the oxidation. Due to the complicated nature of this system, simulations were limited to that of the oxidation of Process 1 at high concentrations of [Pt{((*p*-HC_6F_4)NCH_2)$_2$}(py)$_2$] (A in Scheme 1) on a GC electrode. Under these conditions, many of the voltammetric features could be approximately simulated using the mechanism given in Scheme 1, which includes the formation of two structurally different dimeric platinum species, AB and AB1. All electron transfer processes in the simulation were assumed to be extremely fast, and hence reversible on the voltammetric timescale. $E_{½}$ values given in Scheme 1 are the reversible potentials for the designated electron transfer reaction. For the homogeneous reactions, K_{eq} is the equilibrium constant and k_f and k_b are the associated rate constants (where $K_{eq} = k_f/k_b$) with all parameters having appropriate units. Fig. 10 illustrates the simulated data, which account for the crossover of current, the diminuation of peak height for Process 1 when potential is cycled over the region encompassing Processes 1 and 5, and the relatively small loss of Process 1 when the potential range encompasses Processes 1, 5 and 6. However, it does not account for the steady state nature of Process 5, nor the fact that the first cycle for Process 6 is distinctly different from subsequent cycles.

According to the simulated mechanism, oxidation of [Pt{((*p*-HC_6F_4)NCH_2)$_2$}(py)$_2$], A, occurs with the formation of the mono-oxidised species B, which immediately dimerises to give the multinuclear species, AB. The dimeric species, AB, then undergoes slow rearrangement to form AB1. It is this slow kinetic step that causes the crossover (as seen in Fig. 3 and simulated in Fig. 9). AB1 can then be further oxidised to BB1, or reduced to A_2 which dissociates to give two equivalents of A. This latter pathway enables recovery of [Pt{((*p*-HC_6F_4)NCH_2)$_2$}(py)$_2$] when the potential is cycled over the range encompassing Processes 1, 5 and 6. Remembering that the simulation can only account for the major voltammetric features, further clarification of this mechanism requires the combination of all of the above spectroscopic and voltammetric data and further discussion.

$A = B + e^-$	$E_{½} = 0.07$ V
$A + B = AB$	$K_{eq} = 1 \times 10^6$, $k_f = 1 \times 10^6$, $k_b = 1$
$AB = AB1$	$K_{eq} = 1 \times 10^6$, $k_f = 10$, $k_b = 1 \times 10^{-5}$
$AB1 = BB1 + e^-$	$E_{½} = -0.79$ V
$A_2 = AB1 + e^-$	$E_{½} = -2.35$ V
$A_2 = 2\ A$	$K_{eq} = 7.924 \times 10^{28}$, $k_f = 1 \times 10^6$, $k_b = 1.262 \times 10^{-23}$

Scheme 1

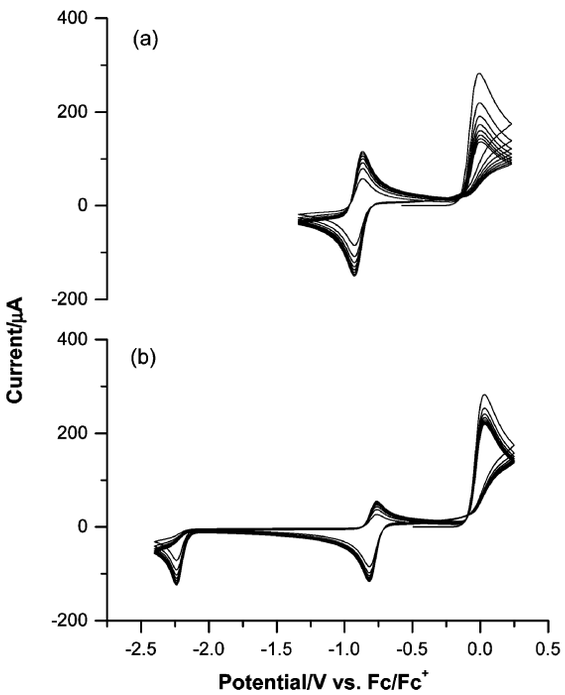

Fig. 10 Simulated cyclic voltammograms at a 1.3 mm radius electrode (with semi-infinite diffusion) of a 10 mM solution at 25 °C (with pre-equilibrium disabled and using diffusion coefficient of 1×10^{-5} cm^2 s^{-1}). Using an initial potential of −500 mV, a scan rate of 1000 mV s^{-1} and scanning for 8 cycles of potential. (a) Switching potential at −1200 mV. (b) Switching potential at −2400 mV.

Proposed mechanism

It is not unusual to find irreversible oxidative electrochemistry associated with Pt(II) complexes, as the square planar platinum(II) can readily accept two additional donors (*e.g.* solvent) following oxidation to give stable platinum(IV) complexes or transient platinum(III) species.[35,36] However, in the present case, lack of substantial electrochemical or spectroscopic difference when the solvent was changed from acetone to acetonitrile renders unlikely the hypothesis that the fast follow-up reaction includes coordination of solvent.

OTTLE experiments suggest that the one-electron oxidation of [Pt{((*p*-HC_6F_4)NCH_2)$_2$}(py)$_2$] is partially chemically reversible, with recovery of a substantial amount of the initial spectrum on re-reduction. This reversibility suggests that under these conditions, all ligands remain coordinated to the platinum throughout the oxidation because if the ligands were to dissociate, the reversibility of the system would be compromised. Similarly, recovery of significant concentrations of [Pt{((*p*-HC_6F_4)-NCH_2)$_2$}(py)$_2$] is possible when voltammograms are obtained immediately following oxidation by one equivalent NO^+ or by BE of ≤ 1 mM concentrations. The use of these low concentrations appears to play a key role in the reversibility of the system.

Interestingly, Process 5 is never observed in voltammograms obtained following BE or chemical oxidation experiments, and [Pt{((*p*-HC_6F_4)NCH_2)$_2$}(py)$_2$] cannot be recovered after long timescale oxidative experiments. This suggests there are differences between the mechanisms observed on the short (voltammetric) and longer timescales.

(a) Short (voltammetric) timescale. The initial step in the oxidation of [Pt{((*p*-HC_6F_4)NCH_2)$_2$}(py)$_2$] is highly likely to be the formation of an isoconnected paramagnetic cation radical, [Pt{((*p*-HC_6F_4)NCH_2)$_2$}(py)$_2$]$^+$, B (Scheme 2). However, B is not detected even on short timescale voltammetric experiments up to a scan rate of 5000 mV s^{-1}. This suggests that this species reacts very rapidly either by dimerisation, or by reaction with [Pt{((*p*-HC_6F_4)NCH_2)$_2$}(py)$_2$]. This latter pathway forms the basis of the initial step in Scheme 1.

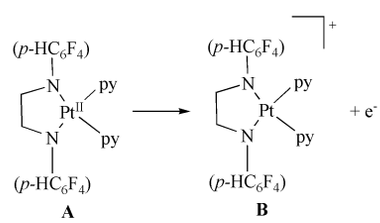

Scheme 2

The most probable dinuclear product of the oxidation of [Pt{((*p*-HC_6F_4)NCH_2)$_2$}(py)$_2$] is one containing bridging μ-organoamide ligands (AB in Scheme 3). Similar bridging by an organoamide nitrogen can be found in the dimeric palladium complexes, [(PdX{(*p*-YC_6F_4)$N(CH_2)_2NR_2$})$_2$] (where R = Me or Et; Y = H or F; X = Cl, Br, I or O_2CPh), with two of the complexes (R = Et; Y = F; X = Cl or O_2CPh) structurally authenticated by single crystal X-ray diffraction techniques.[37,38]

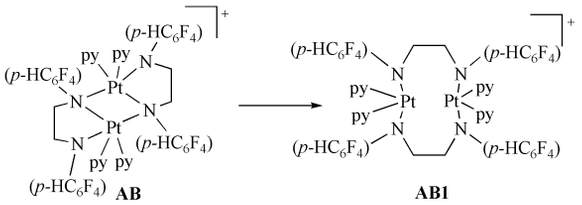

Scheme 3

However, unlike the palladium species, the μ-organoamide coordination results in 5-coordintate platinum metal centres, with the fluorocarbon rings and pyridines presumably in close proximity, introducing an amount of strain into the system. Alleviation of this strain can be achieved by breaking two of the Pt–N bonds (as in Scheme 3) to form a dinuclear platinum complex with bridging organoamide ligands (AB1 in Scheme 3). This rearrangement agrees with the proposed voltammetric mechanism, which requires the existence of at least two structurally unique dinuclear complexes, AB and AB1, where AB1 is formed by a chemical step from AB. Not only is this new complex radical likely to be more stable than the sterically hindered dinuclear radical, but it allows for the slow kinetic step in the mechanism of the simulation. The new platinum dinuclear complex, AB1, is able to undergo further oxidation to give a diradical complex, BB1, or be reduced back to a platinum(II) analogue, A_2, which immediately rearranges to give two equivalents of [Pt{((*p*-HC_6F_4)NCH_2)$_2$}(py)$_2$] (see Scheme 4).

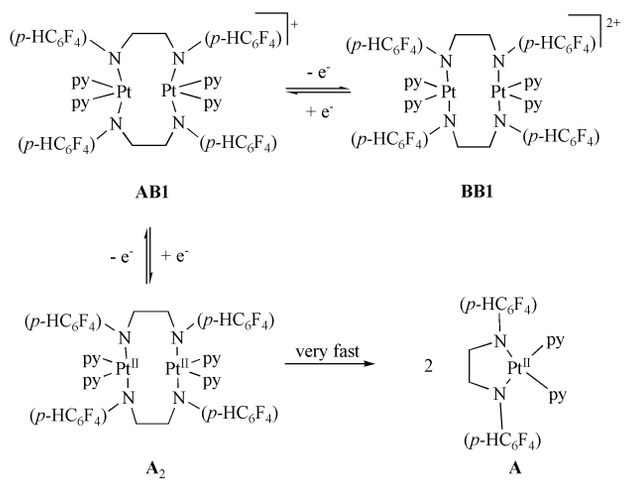

Scheme 4

It must be noted that the proposed formation of dinuclear platinum species is the simplest mechanism, and formation of oligomeric platinum complexes are also possible. It must be remembered that whilst it explains many of the features, Scheme 1 does not fully explain all features of the cyclic voltammetry. Under conditions where high concentrations of B are formed, Scheme 5, which generates a Pt^{III}–Pt^{III} complex, is likely to contribute to the voltammetry.

(b) Long timescale. On longer timescale, high concentration experiments, formation of different products are probable.

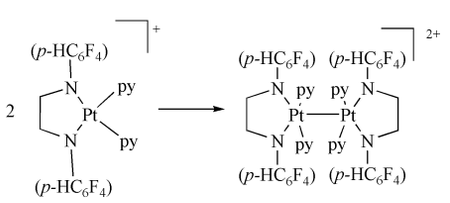

Scheme 5

Although the initial step in the oxidation is identical to that on the short timescale (Scheme 2), the nature of the follow-up reactions appears to vary considerably with reaction conditions.

Partial oxidation of very high concentrations (50 mM) of [Pt{((*p*-HC_6F_4)NCH_2)$_2$}(py)$_2$] leads to the detection of an EPR active species. The voltammetric evidence relevant to these conditions suggest that this moderately stable species is not monomeric, although it is impossible to tell by the EPR spectrum whether the active species is monomeric, dinuclear or oligomeric. The use of saturated solutions of [Pt{((*p*-HC_6F_4)-NCH_2)$_2$}(py)$_2$] coupled with the generation of small amounts of [Pt{((*p*-HC_6F_4)NCH_2)$_2$}(py)$_2$]$^+$ favours reaction to give EPR active species such as AB, AB1 (see Scheme 3) or **4** in which the oxidised organoamide ligand is chelated to one Pt centre. There is no evidence from EPR spectroscopy of the oxidised ligand bridging two equivalent Pt centres.

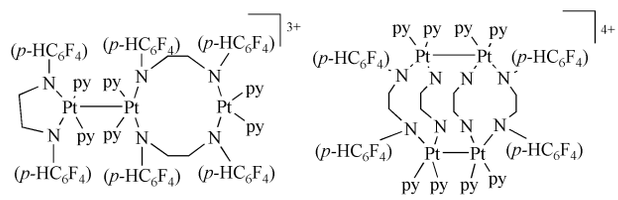

4 **5**

(Some fluorocarbons omitted for clarity)

At very high concentrations of B (for example, immediately following oxidation by one equivalent of NO^+), the unstable radical cation is more likely to dimerise with itself, which could give rise to the formation of a platinum(III) dimer containing an unsupported Pt–Pt bond, BB2 (Scheme 5). Oligomerisation by further reaction with [Pt{((*p*-HC_6F_4)NCH_2)$_2$}(py)$_2$]$^+$ is also possible, and **4** and **5** are examples of possible oligomers.

NMR spectroscopy following oxidation of high concentrations (10 mM) of [Pt{((*p*-HC_6F_4)NCH_2)$_2$}(py)$_2$] confirms that all ligands remain attached to the platinum in the expected ratios (free pyridine or free protonated organoamide ligand were only detected in aged solutions), and suggests that the complex remains symmetrical. In order for the complex to be diamagnetic following a one-electron oxidation, there must be electron pairing and the most feasible solution is the inclusion of a Pt–Pt bond (as in BB2 in Scheme 5, BB3 in Scheme 6), particularly as there is no NMR spectroscopic evidence of ligand decomposition or dissociation, or any unusual ligand coordination immediately after oxidation. In addition, the reaction of BB1 to BB3 can account for the lack of Process 5 following BE or chemical oxidation, as the complex containing the Pt–Pt bond (BB3) is likely to be more stable than the diradical complex, BB1.

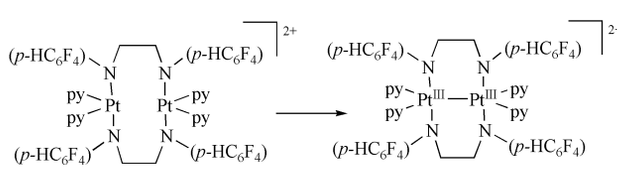

Scheme 6

Unfortunately, attempts to crystallise the mono-oxidised product have proven unsuccessful, so an unequivocal structural determination is not possible. However, the list of dinuclear platinum(III) complexes containing a Pt–Pt bond has been rapidly expanding in the last decade,[39] in contrast to the relatively rare monomeric platinum(III) complexes.[40–44] Consequently, this knowledge coupled with the spectroscopic data presented here (including ESMS results), supports the formation of a platinum(III) dimer or oligimer as the major product

of one-electron oxidation on the long timescale. Most reported dimeric platinum(III) complexes have bridging ligands of appropriate bite (*e.g.* amides,[45–47] acetates[48] and thioacetates,[49] nucleobases,[50–52] sulfates,[53] phosphates[54] and diphosphites[55]), although there are a number of dinuclear platinum(III) compounds with no bridging ligands,[56–59] which lends support to the proposed intermediates above.

Interestingly, any number of platinum(III) oligomers could be possible oxidation products, as long as the resulting complex is diamagnetic and symmetrical (pyridines and the flurocarbons in equivalent environments respectively).

Formation of platinum(IV) complexes

Despite the inherent complexity associated with the range of complexes formed by a one-electron oxidation, the second one-electron step seems to always occur at a similar potential and give the same products (compare Figs. 4 and 5). Note the close similarity of Processes 2, 7 and 8 to Processes 9, 10 and 11.

The one-electron oxidation of the platinum(III) complexes logically produces a 6-coordinate platinum(IV) complex, void of any Pt–Pt bond. A plausible structure would contain solvent or electrolyte in the 5th and 6th coordination positions to give a structure of the kind shown in **6**. This particular structure does not allow reduction back to the initial organoamidoplatinum(II) complex, [Pt{((*p*-HC_6F_4)NCH_2)$_2$}(py)$_2$].

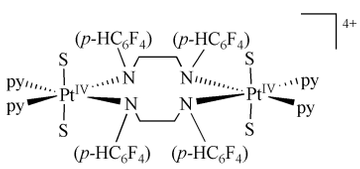

6

S = solvent or electrolyte

It is intriguing to note that reaction of [Pt{((*p*-HC_6F_4)-NCH_2)$_2$}(py)$_2$] with hydrogen peroxide produces the dihydroxoplatinum(IV) analogue, [Pt{((*p*-HC_6F_4)NCH_2)$_2$}(py)$_2$(OH)$_2$], *via* what is apparently an overall oxidative addition reaction.[17] The data in this work suggest that in the absence of reasonably good coordinating ligands, the formation of moderately stable platinum(III) complexes occur. That is, the excellent coordination ability of hydroxide as a ligand when H_2O_2 is used as an oxidant appears to lead to a very different reaction pathway and types of products relative to the case when NO^+ or electrochemistry is used to achieve oxidation.

Conclusions

The oxidation of [Pt{((*p*-HC_6F_4)NCH_2)$_2$}(py)$_2$], under voltammetric conditions at reasonable concentration, occurs *via* two well separated one-electron processes, rather than a single two-electron step, as is commonly observed in oxidative platinum chemistry. On long timescale experiments, diamagnetic supported platinum(III) dinuclear or oligomeric complexes are formed which can, in turn, be oxidised to the platinum(IV) state. A mechanism for the initial one-electron oxidation can be proposed on the basis of voltammetric and spectroelectrochemical data.

Acknowledgements

The authors gratefully acknowledge Stephen Feldberg for assistance with the simulation of the cyclic voltammetry and for valuable discussions over the duration of this project. The authors also thank Susan Turland for providing a sample of [Pt{((*p*-HC_6F_4)NCH_2)$_2$}(py)$_2$(OH)$_2$]. This work is in part a contribution from the Edinburgh Protein Interaction Centre funded by the Wellcome Trust. The authors thank Dr E. J. L. McInnes of the EPSRC multicentre EPR service in Manchester for frozen glass EPR simulations.

References

1 G. B. Deacon, B. M. Gatehouse, I. L. Grayson and M. C. Nesbit, *Polyhedron*, 1984, **3**, 753.
2 D. P. Buxton, G. B. Deacon, B. M. Gatehouse, I. L. Grayson, R. J. Thomson and D. S. C. Black, *Aust. J. Chem.*, 1986, **39**, 2013.
3 G. W. Watt and D. G. Upchurch, *J. Am. Chem. Soc.*, 1968, **90**, 914.
4 G. W. Watt and J. E. Cuddeback, *Inorg. Chem.*, 1971, **10**, 947.
5 L. K. Webster, A. G. Ellis, C. Apicella and G. B. Deacon, *Cancer Chemother. Pharmacol.*, 2002, **49**, 87.
6 T. Talarico, C. M. Cullinane, P. J. Gray, L. K. Webster, G. B. Deacon and D. R. Phillips, *Anti-Cancer Drug Des.*, 2001, **16**, 135.
7 M. J. Bloemink, R. J. Heetebrij, J. Ireland, G. B. Deacon and J. Reedijk, *JBIC, J. Biol. Inorg. Chem.*, 1996, **1**, 278.
8 T. Talarico, D. R. Phillips, G. B. Deacon, S. Rainone and L. K. Webster, *Invest. New Drugs*, 1999, **17**, 1.
9 L. K. Webster, G. B. Deacon, D. P. Buxton, B. L. Hillcoat, A. M. James, I. A. G. Roos, R. J. Thomson, L. P. G. Wakelin and T. L. Williams, *J. Med. Chem.*, 1992, **35**, 3349.
10 E. Wong and C. M. Giandomenico, *Chem. Rev. (Washington, D. C.)*, 1999, **99**, 2451.
11 T. W. Hambley, *Coord. Chem. Rev.*, 1997, **166**, 181.
12 T. W. Hambley, A. R. Battle, G. B. Deacon, E. T. Lawrenz, G. D. Fallon, B. M. Gatehouse, L. K. Webster and S. Rainone, *J. Inorg. Biochem.*, 1999, **77**, 3.
13 G. B. Deacon, E. T. Lawrenz, T. W. Hambley, S. Rainone and L. K. Webster, *J. Organomet. Chem.*, 1995, **493**, 205.
14 C. M. Giandomenico, M. J. Abrams, B. A. Murrer, J. F. Vollano, M. I. Reheinheimer, S. B. Wyer, G. E. Bossard and J. D. Higgins, *Inorg. Chem.*, 1995, **34**, 1015.
15 C. F. J. Barnard, J. F. Vollano, P. A. Chaloner and S. Z. Dewa, *Inorg. Chem.*, 1996, **35**, 3280.
16 G. B. Deacon, B. M. Gatehouse, S. T. Haubrich, J. Ireland and E. T. Lawrenz, *Polyhedron*, 1998, **17**, 791.
17 A. R. Battle, G. B. Deacon, G. Fallon, B. M. Gatehouse, T. W. Hambley, E. T. Lawrenz, L. C. Kelly, S. Rainone, L. K. Webster, J. M. Miller, manuscript in preparation.
18 P. T. Kissinger, W. R. Heineman, *Laboratory Techniques in Electroanalytical Chemistry*, Marcel Dekker, Inc., New York, 1984.
19 WINEPR Simfonia, Version 1.25, Bruker Analytische Messtechnik GmbH, Rheinstetten/Karlsruhe, Germany, 1996.
20 DigiSim for Windows 95, Version 3.05, Bioanalytical Systems Inc, Indiana, USA, 2000.
21 L. M. Mink, J. W. Voce, J. E. Ingersoll, V. T. Nguyen, R. K. Boggess, H. Washburn and D. I. Grove, *Polyhedron*, 2000, **19**, 1057.
22 J. J. Comerford, PhD Thesis, Melbourne University, 2001.
23 D. C. Harris M. D. Bertolucci, *Symmetry and spectroscopy: An Introduction to vibrational and electronic spectroscopy*, Oxford University Press, New York, 1978.
24 D. V. Stynes, *Inorg. Chem.*, 1975, **14**, 453.
25 S. Turland, unpublished work.
26 D. Buxton, PhD Thesis, Monash University, 1986.
27 W. Clegg, *J. Chem. Soc., Dalton Trans.*, 1993, 3453.
28 M. Watabe, *Inorg. Chem.*, 2001, **40**, 1496.
29 P. S. Pregosin, *Annu. Rep. NMR Spectrosc.*, 1986, **17**, 285.
30 P. S. Pregosin, *Coord. Chem. Rev.*, 1982, **44**, 241.
31 R. J. Goodfellow, in *Multinuclear NMR*, ed. J. Mason, Plenum Press, New York, 1989.
32 G. Wagner, *Inorg. Chem.*, 2001, **40**, 1683.
33 M. Rashidi, *J. Organomet. Chem.*, 2001, **633**, 105.
34 K. O. Christe, D. A. Dixon, G. J. Schrobilgen and W. W. Wilson, *J. Am. Chem. Soc.*, 1997, **119**, 3918.
35 L. Johansson, O. B. Ryan, C. Romming and M. Tilset, *Organometallics*, 1998, **17**, 3957.
36 M. Crespo, C. Grande and A. Klein, *J. Chem. Soc., Dalton Trans.*, 1999, 1629.
37 D. Mason, unpublished work.
38 W. Ingram, PhD Thesis, Monash University, 1997.
39 G. Natile, F. P. Intini and C. Pacifico, *Cisplatin*, 1999, 429.
40 H. A. Boucher, G. A. Lawrance, P. A. Lay, A. M. Sargeson, A. M. Bond, D. F. Sangster and J. C. Sullivan, *J. Am. Chem. Soc.*, 1983, **105**, 4652.
41 T. V. O'Halloran and S. J. Lippard, *Isr. J. Chem.*, 1985, **25**, 130.
42 J. Fornies, B. Menjon, R. M. Sanz-Carrillo, M. Tomas, N. G. Connelly, J. G. Crossley and A. G. Orpen, *J. Am. Chem. Soc.*, 1995, **117**, 4295.

43 P. R. Boutchev, M. Meteva and G. Gentcheva, *Pure Appl. Chem.*, 1989, **61**, 897.
44 A. J. Blake, R. O. Gould, A. J. Holder, T. I. Hyde, A. J. Lavery, M. O. Odulate and M. Schroder, *J. Chem. Soc., Chem. Commun.*, 1987, 118.
45 S. J. Lippard and L. S. Hollis, *J. Am. Chem. Soc.*, 1981, **103**, 6761.
46 T. V. O'Halloran, M. M. Roberts and S. J. Lippard, *Inorg. Chem.*, 1986, **25**, 957.
47 K. Matsumoto and K. Harashima, *Inorg. Chem.*, 1991, **30**, 3032.
48 T. G. Appleton, K. J. Barnham, K. A. Byriel, J. R. Hall, C. H. L. Kennard, M. T. Mathieson and K. G. Penman, *Inorg. Chem.*, 1995, **34**, 6040.
49 C. Bellitto, G. Dessy, V. Fares and A. Flamini, *Congr. Naz. Chim. Inorg., [Atti], 16th*, 1983, 138.
50 B. Lippert, *New J. Chem.*, 1988, **12**, 715.
51 M. Peilert, S. Weissbach, E. Freisinger, V. I. Korsunsky and B. Lippert, *Inorg. Chim. Acta*, 1997, **265**, 187.
52 H. Schoellhorn, P. Eisenmann, U. Thewalt and B. Lippert, *Inorg. Chem.*, 1986, **25**, 3384.
53 F. A. Cotton, S. Falvello and S. Han, *Inorg. Chem.*, 1982, **21**, 2889.
54 R. El-Mehdawi, F. R. Fronczek and D. M. Roundhill, *Inorg. Chem.*, 1986, **25**, 1155.
55 C. M. Che, W.-M. Lee, T. C. W. Mak and H. B. Gray, *J. Am. Chem. Soc.*, 1986, **108**, 4446.
56 R. Cini, F. P. Fanizzi, F. P. Intini and G. Natile, *J. Am. Chem. Soc.*, 1991, **113**, 7805.
57 L. A. M. Baxter, G. A. Heath, R. G. Raptis and A. C. Willis, *J. Am. Chem. Soc.*, 1992, **114**, 6944.
58 G. Bandoli, P. A. Caputo, F. P. Intini, M. F. Sivo and G. Natile, *J. Am. Chem. Soc.*, 1997, **119**, 10370.
59 P. D. Prenzler, G. A. Heath, S. B. Lee and R. G. Raptis, *Chem. Commun.*, 1996, 2271.